XIX Int. Conf. on
High Energy Physi
Aug. 1978, Tokyo
Japan

Topological Cross Sections for K^+p Interactions at 147 GeV/c*

D. Brick, A. M. Shapiro
Brown University, Providence, Rhode Island 02912

R. Ansorge, B. Whyman
Cambridge University, Cambridge, England

F. Bruyant, L. Montanet
CERN, Geneva, Switzerland

R. A. Burnstein, H. Rubin
Illinois Institute of Technology, Chicago, Illinois 60616

J. Cooper, R. D. Sard
University of Illinois, Urbana, Illinois 61801

L. Bachman, A. Pevsner
The Johns Hopkins University, Baltimore, Maryland 21218

E. S. Hafen, I. A. Pless
Massachusetts Institute of Technology, Cambridge, Massachusetts 02139

F. Grard, R. Windmolders
University of Mons, Mons, Belgium

B. DeBock, M. Schouten
University of Nijemgen, Nijmegen, The Netherlands

H. O. Cohn
Oak Ridge National Laboratory, Oak Ridge, Tennessee 37830

L. Ventura, G. Zumerle
University of Padova, Padova, Italy

E. Calligarich, S. Ratti
University of Pavia, Pavia, Italy

G. Bressi, D. Zanello
University of Roma, Rome, Italy

T. C. Ou, R. J. Plano
Rutgers University, New Brunswick, New Jersey 08903

E. B. Brucker, S. Taylor
Stevens Institute of Technology, Hoboken, New Jersey 07030

J. Goldberg, S. Toaff
Technion, Haifa, Israel

A. Levy, Y. Oren
University of Tel Aviv, Tel Aviv, Israel

G. Condo, E. Hart
University of Tennessee, Knoxville, Tennessee 37916

E. Castelli, M. Sessa
University of Trieste, Trieste, Italy

D. Hochman, U. Karshon
Weizmann Institute of Science, Rehovot, Israel

D. Ljung, T. Ludlam
Yale University, New Haven, Connecticut 06520

*Work supported in part by U.S. DOE, U.S. NSF, U.S.-Israel BSF, Italian INFN and Dutch FOM-ZWO.

Abstract

The Fermilab Hybrid 30" Bubble Chamber Spectrometer was exposed to a tagged 147 GeV/c positive beam containing π^+, K^+ and p. A sample of 1572 K^+p interactions is used to derive σ_{top}, $\langle n_c \rangle$, f_2^{cc} and $\langle n_c \rangle / D$ values. For comparison similar data are presented for 8931 pp interactions and 10257 π^+p interactions. In addition a comparison is made with similar data from a negative beam at the same momentum[1].

1 D. Fong et al., Nuc. Physics B102 (1976) 386.

We present data on the topological cross sections for K^+p, π^+p and pp interactions at 147 GeV/c in the FNAL 30-inch Hybrid Spectrometer. These data come from approximately one-third of a 430,000 picture exposure of the 30-inch chamber to an unseparated beam of positive particles.

The particle identities were determined by means of Čerenkov counters[1] upstream of the bubble chamber. Three triples of multiwire proportional chambers (PWC) upstream of the chamber were used to associate the Čerenkov tag with an interaction vertex within the chamber (Time Slot). To determine the vertex coordinates we have used only those events that have been precision measured by automatic machines and have been reconstructed[2]. Approximately 11% of the vertex measurements could not be associated with a Čerenkov tag (No Time Slot), mainly because two beam tracks are too close to be resolved with confidence. We assume that the No Time Slot rejects are unbiased as to particle type.

In Table I we show the total number of events that have a Time Slot. For the rolls of film used in this analysis we have processed the PWC tapes to determine the beam composition as shown in the table. The "junk" represents either incomplete or inconsistent status bits for the particle tag and may represent electronic noise. In addition, we have determined the elastic scatters from an even smaller subset of the data [see Ref. 1 for a description of the technique used].

Because of the incomplete nature of the data, it has been necessary at this stage to normalize our cross sections. Since there exists[3] determinations of the topological cross sections

for pp interactions up to 400 GeV/c but nothing above 100 GeV/c for either π^+p or K^+p interactions, we have chosen a single normalization to the pp total cross section, $\sigma_{Tot}(pp)$ only. All other cross sections are then determined by using

$$\sigma_{Tot}\ (\pi/K) = \frac{N'(\pi/K)}{N'(p)} \cdot \frac{B'(p)}{B'(\pi/K)}\ \sigma_{Tot}\ (pp)$$

where $N'(\pi/K)$ and $N'(p)$ are the corrected numbers of interactions for each beam particle (π, K or p) and B' is the total beam corrected for attenuation for each beam particle. Since we are normalizing the data to σ_{Tot} (pp) many corrections which normally are made to a data sample may now be ignored.

The scan efficiency for two-prong interactions was 93.5% as compared to 98.2% for all other interactions. Therefore the two prongs found are corrected for relative losses by 5%. For the inelastic two-prongs an additional 5% correction has been applied to correct for azimuthal losses. For the fraction of events assumed to be elastic scatters an additional low $|t|$ correction has been applied ($\sim$20%) as determined from the $|t|$ distributions of the measured elastic scatters.

Because the data sample comes from the measurement of complete events the more complicated events (high multiplicities) tend to exceed the available computer memory and are rejected. These rejects have been distributed between π, K and proton in a given topology in the same ratio as the "good" events. These corrections ranged from 4% for 8-prongs to 150% for 18-prongs.

Corrections, as a function of multiplicity were applied for close in neutral vertices and close in scatters that were not detected. These corrections averaged ~0.2%.

The elastic and total cross sections as determined by the above procedure are listed in Table II. For comparison the counter results[4] are given as well as the results for π^-p and K^-p interactions at 147 GeV/c as determined in a previous experiment[5]. The agreement between this experiment and Carroll et al for the various σ_{Tot} lends credence to the procedure of assigning the rejected events. Essentially the same total cross sections could have been obtained without using any corrections since the total corrections were within 1% of each other. The topological cross sections for the pp interactions are listed in Table III and displayed on Fig. 1 which also contains the results at other momenta[6]. Our data is consistent with the compilation.

The topological cross sections for the π^+p interactions are listed in Table IV. For comparison we also list in this table the π^-p topological cross sections at 147 GeV/c from Ref. 5. The π^+p cross sections are displayed in Fig. 2 with the published results at lower momenta[6]. The decrease in the 4-prong cross section with increasing p_{lab} is maintained at our higher momenta. The 6 and 8-prong cross section appear to be decreasing or, at least, have reached a plateau at the energy of this experiment. The inclusion of our higher momentum 2-prong cross section indicates that this cross section is still decreasing as denoted by the dashed curve.

The topological cross sections for the K^+p interactions are listed in Table V. Again for comparison we list the K^-p cross sections from Ref. 5. The K^+p results are displayed in Fig. 3 along with the published values obtained at lower momenta[7]. The lack of high momentum data points indicates clearly the difficulties of working with unseparated beams. Although our data is preliminary it still contains almost seven times the number of events of the next lower momentum. The solid lines in Fig. 3 are drawn to aid the eye. The trends established by the improved statistics of this experiment are similar to those seen in the π^+p interactions in that the inelastic 2 prong cross section in less than the value measured at 32 GeV/c and the 6 and 8-prong cross section appear to have least reached a plateau.

We have calculated a few of the statistical moments for our topological cross sections. These values are listed in Table VI. In this table we also list the moments for the π^-p and K^-p cross sections from Ref. 5. We display these results on the compendium of J. Whitmore[6] in Fig. 4. The moments from this experiment show the same general trends as the rest of the data. We have fitted $\langle n \rangle$ for the K^+p interactions with $p_{lab} \geq 3.5$ GeV/c, as a function of incident momentum, to both linear and quadratic forms in ln s,

$$\langle n \rangle = a + b \ln s$$

$$\langle n \rangle = a + b \ln s + c \ln^2 s$$

with the following results:

$$\langle n \rangle = (0.00 \pm 0.05) + (1.25 \pm 0.02) \ln s$$

$$\chi^2/\text{NDF} = 45.4/6, \text{ C.L.} < 10^{-4}$$

and

$$\langle n \rangle = (1.05 \pm 0.17) + (0.56 \pm 0.11) \ln s + (0.10 \pm 0.02) \ln^2 s$$

$$\chi^2/\text{NDF} = 3.81/5, \text{ C.L.} = 0.60$$

The addition of our data at 147 GeV/c is sufficient to discriminate against the linear dependence on ln s. In order to better compare with pp and π^-p data we have also fit to the form

$$\langle n \rangle = a + b \ln E_a + c \ln^2 E_a$$

where E_a is the available energy, $E_a = \sqrt{s} - (M_K + M_p)$, as suggested by Whitmore[3]. The results of this fit are:

$$\langle n \rangle = (2.40 \pm 0.04) + (0.61 \pm 0.08) \ln E_a + (0.45 \pm 0.03) \ln^2 E_a$$

$$\chi^2/\text{NDF} = 3.55/5, \text{ C.L.} = 0.72$$

The coefficients for the fit[3] to π^-p and pp interactions up to 400 GeV/c are: a = 2.45, b = 0.32 and c = 0.53. Apparently the presence of a strange quark in K^+p interactions has little effect on the energy dependence of the average charged multiplicity. We display in Fig. 5 the data along with the linear ln s result (dashed curve) and the best fit to E_a (solid curve).

Finally, in Fig. 6, we display the topological cross sections in the KNO scaling form for $K^\pm$p, $\pi^\pm$p and pp interactions at 147 GeV/c. The five reactions are similar to each other and follow closely Slattery's empirical fit[8] to the data for pp collisions between 50 and 300 GeV/c (solid curve).

References

1. D. Fong, et al., Physics Letters 53B (1974) 290.
2. The reconstruction chains were:

   PRECIS - GEOHYB for the Northern European groups

   GEOMAT - PWGP - TKORG for the United States groups.
3. J. Whitmore, Physics Reports 10C (1974) 273;

   J. Whitmore, Physics Reports 27C (1976) 187.
4. Carroll, et al., Phys. Rev. Letters 33 (1974) 932;

   Carroll, et al., Phys. Rev. Letters 33 (1974) 928;

   Ayres, et al., Phys. Rev. D15 (1977) 3105.
5. D. Fong, et al., Physics Letters 53B (1976) 386.
6. Figures 1, 2 and 4 are from Ref. 3 with our results added. Copies of these drawings were graciously supplied to us by J. Whitmore.
7. 5, 8.25 and 16 GeV/c: R. Windmolders, private communication; 12.7 GeV/c: S. L. Stone et al., Nuc. Phys. B32 (1971) 19; 32 GeV/c: G. A. Akopdjanov et al., Nuc. Phys. B75 (1974) 401; 100 GeV/c: V. E. Barnes et al., Phys. Rev. Letters 34 (1975) 415.
8. P. Slattery, Phys. Rev. Letters 29 (1972) 1624.

Figure Captions

Figure 1 — pp Topological Cross Sections
The solid curves are to guide the eye. The arrow locates this experiment.

Figure 2 — π^+p Topological Cross Sections
The arrow locates this experiment.

Figure 3 — K^+p Topological Cross Sections
The arrow locates this experiment.

Figure 4 — (a) Average charged multiplicity, (b) $\langle n \rangle$/Dispersion, and (c) f_2^{cc} as a function of incident beam momentum for $\pi^\pm p$, $K^\pm p$ and $p^\pm p$ interactions.

Figure 5 — $\langle n \rangle$ as a function of beam momentum. See text for an explanation of the curves.

Figure 6 — The KNO scaling function $\langle n \rangle \frac{\sigma_n}{\sigma_{inel}}$ versus $n/\langle n \rangle$ for $K^\pm p$, $\pi^\pm p$ and pp at 147 GeV/c.

Table I

Event Statistics

Beam	Good Events	Elastics[a]	Percent[b] Beam
p	8931	417	30.32
π^+	10257	410	57.24
K^+	1572	62	10.55
junk	---	---	1.89
	20760	889	100.

a) From one-half of data sample used here.

b) Before attenuation correction.

Table II

Total and Elastic Cross Sections at 147 GeV/c

	σ_{Tot} This Experiment	σ_{Tot} Carroll[a] et al	σ_{el} This Experiment	σ_{el} Carroll[a] et al
pp	38.62[b]	38.62±0.06	7.00±0.34	6.99±0.08
π^+p	23.17±0.23	23.46±0.06	3.33±0.11	3.42±0.08
K^+p	19.39±0.44	19.33±0.08	2.44±0.22	2.43±0.09
π^-p[c]	24.24±0.29		3.24±0.14	
K^-p[c]	21.5 ±1.0		2.74±0.42	

a) Ref. 4

b) Normalized to σ_{Tot}(pp) of Ref. 4

c) Results are from Ref. 1.

Table III

Topological Cross Sections in pp Interactions at 147 GeV/c

Number of charged prongs, n	Number of events seen	Corrected number of events	Cross Section, mb
2	2149	2964.6	10.49 ±0.23
	elastic	1978.3	7.00 ±0.34
	inelastic	986.2	3.49 ±0.21
4	1572	1777.6	6.29 ±0.16
6	1770	1965.4	6.95 ±0.17
8	1451	1634.6	5.78 ±0.15
10	1000	1188.3	4.20 ±0.13
12	593	750.9	2.66 ±0.11
14	239	348.7	1.23 ±0.08
16	113	189.8	0.67 ±0.05
18	33	67.2	0.24 ±0.03
20	10	24.6	0.087±0.018
22	-	6.3	0.022±0.009
24	1	1.1	0.004±0.004
Total	8931		38.62
		σ_{inel}	31.62 ±0.35

Table IV

Topological Cross Sections in πp Interactions at 147 GeV/c

Number of charged prongs, n	$\pi^+ p$ (This experiment) Number of events seen	Corrected number of events	Cross section, mb	$\pi^- p$ (Ref. 5) Cross section, mb
2	1938	2693.4	5.03 ±0.13	5.04 ±0.15
	elastic	1783.3	3.33 ±0.14	3.24 ±0.14
	inelastic	910.1	1.70 ±0.08	1.80 ±0.12
4	1737	1951.2	3.64 ±0.09	4.12 ±0.10
6	2040	2246.3	4.19 ±0.09	4.47 ±0.10
8	1897	2149.9	4.01 ±0.09	4.30 ±0.11
10	1338	1574.8	2.94 ±0.08	3.09 ±0.09
12	755	971.2	1.81 ±0.07	1.78 ±0.07
14	348	486.6	0.91 ±0.05	0.83 ±0.05
16	145	233.8	0.44 ±0.04	0.39 ±0.03
18	42	74.6	0.14 ±0.02	0.15 ±0.02
20	12	25.8	0.048±0.014	0.054±0.010
22	5	8.2	0.015±0.007	0.007±0.004
Total	10257		23.17 ±0.23	24.24 ±0.29

Table V

Topological Cross Sections in Kp Interactions at 147 GeV/c

	K^+p (This experiment)			K^-p (Ref. 5)
Number of charged prongs, n	Number of events seen	Corrected number of events	Cross section, mb	Cross section, mb
2	305	409.3	4.13 ±0.24	4.27 ±0.53
	elastic	241.2	2.44 ±0.22	2.74 ±0.42
	inelastic	168.1	1.70 ±0.14	1.53 ±0.32
4	299	337.2	3.41 ±0.20	3.59 ±0.47
6	310	343.5	3.47 ±0.20	4.75 ±0.58
8	286	324.6	3.28 ±0.19	3.27 ±0.47
10	196	232.7	2.35 ±0.17	3.27 ±0.47
12	101	142.8	1.44 ±0.14	1.32 ±0.32
14	49	77.0	0.78 ±0.10	0.47 ±0.21
16	17	36.3	0.37 ±0.07	0.16 ±0.11
18	8	13.2	0.13 ±0.04	0.32 ±0.16
20	–	3.8	0.038±0.022	0.11 ±0.05
22	1	1.2	0.012±0.012	
Total	1572		19.39 ±0.49	21.5 ±1.0

Table VI

Moments of the Multiplicity Distributions at 147 GeV/c

	pp	π^+p	π^-p c)	K^+p	K^-p c)
$\langle n \rangle$	7.23±0.07	7.55±0.05	7.40±0.04	7.37±0.09	7.33±0.21
D a)	3.66±0.08	3.60±0.07	3.54±0.03	3.66±0.15	3.51±0.17
$\langle n \rangle$/D	1.98±0.05	2.10±0.04	2.09±0.02	2.01±0.09	2.09±0.09
f_2^{cc} b)	6.16±0.40	5.41±0.40	5.14±0.22	6.02±0.99	5.0 ±1.1

a) $D = (\langle n^2 \rangle - \langle n \rangle^2)^{1/2}$

b) $f_2^{cc} = \langle n(n-1) \rangle - \langle n \rangle^2$

c) Ref. 5

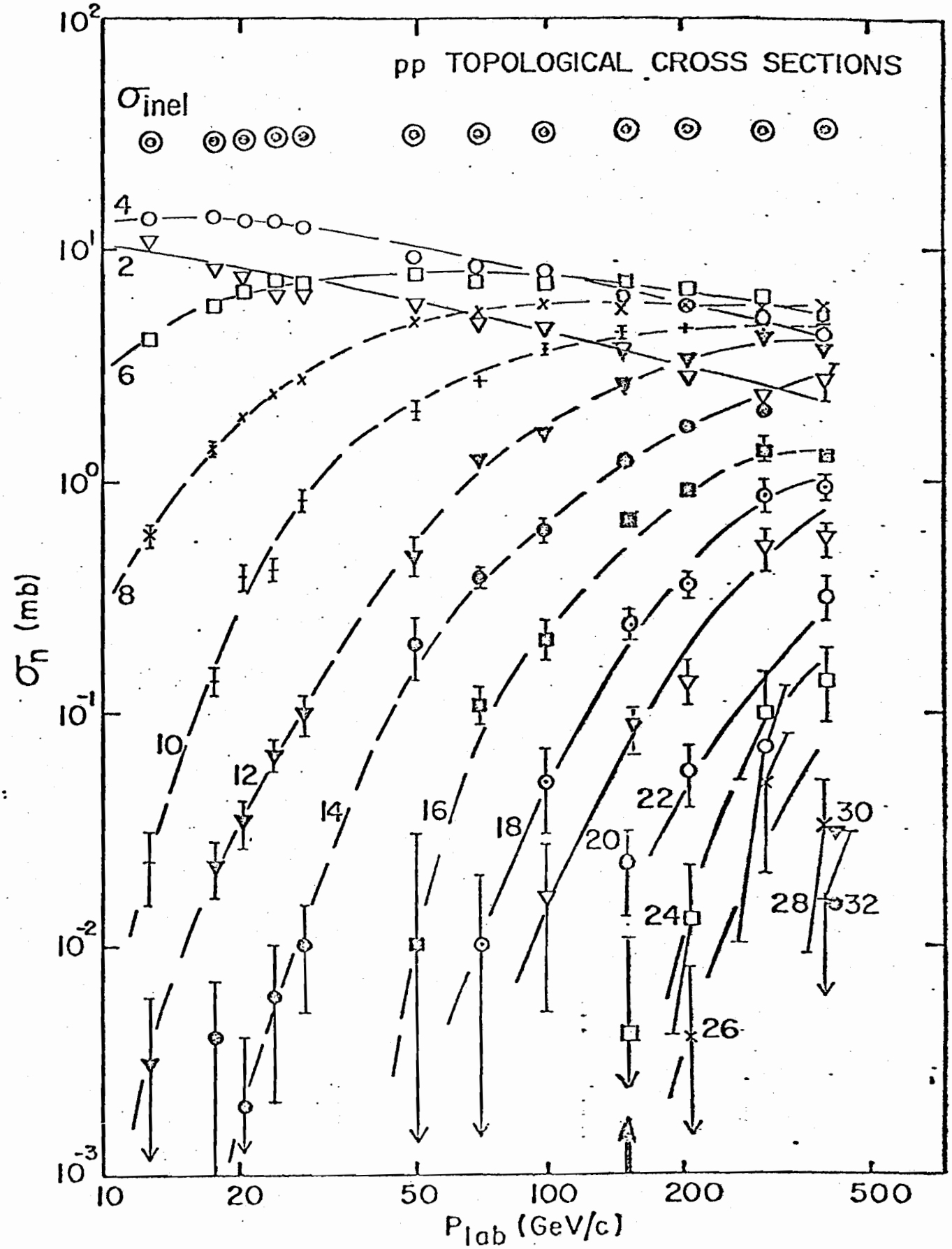
pp TOPOLOGICAL CROSS SECTIONS
σ_{inel}
4
2
6
8
10
12
14
16
18
20
22
24
26
28
30
32
σ_n (mb)
P_{lab} (GeV/c)
10^2
10^1
10^0
10^{-1}
10^{-2}
10^{-3}
10
20
50
100
200
500

Figure 1

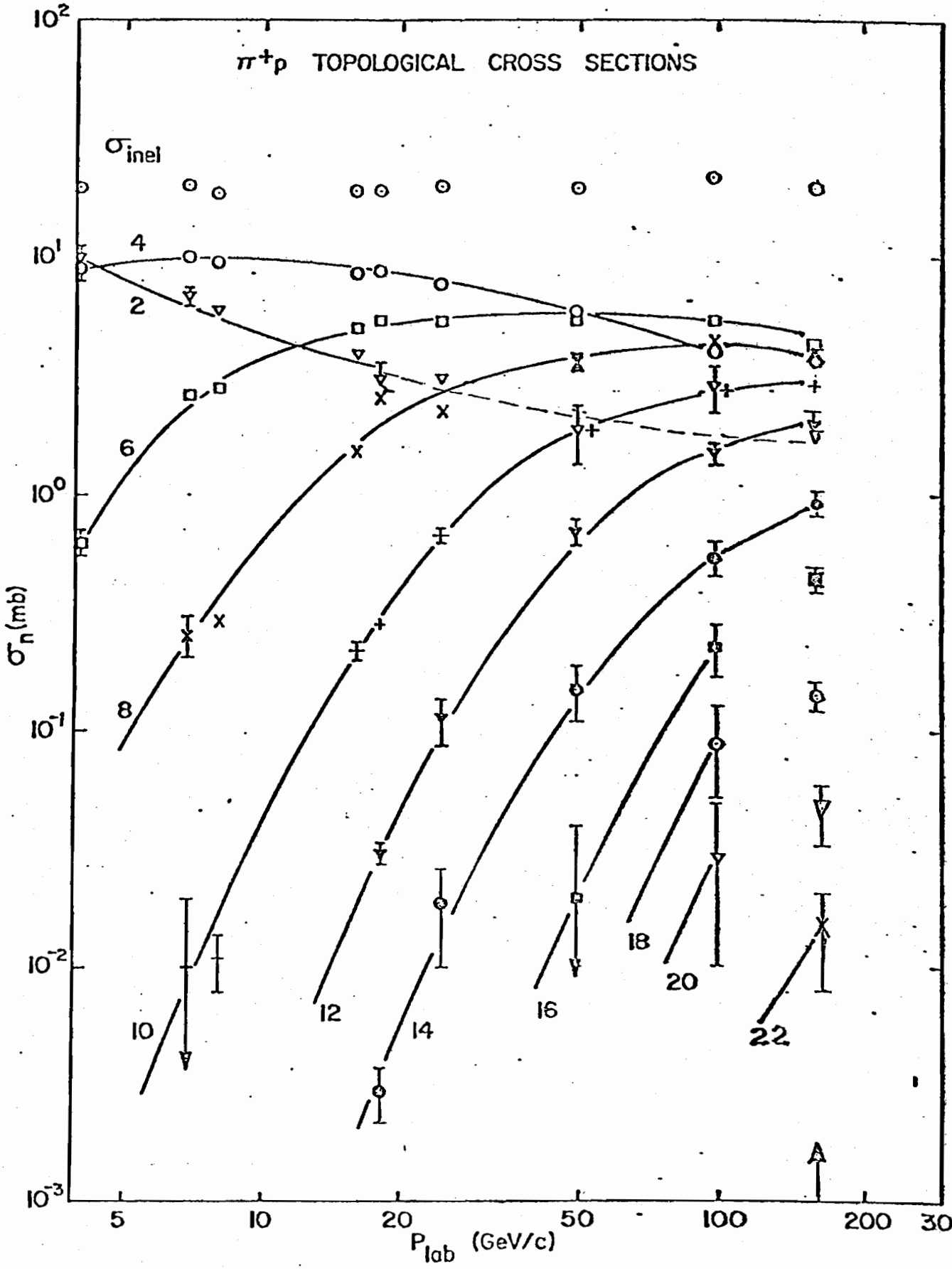
π^+p TOPOLOGICAL CROSS SECTIONS
σ_{inel}
σ_n (mb)
P_{lab} (GeV/c)
10^2
10^1
10^0
10^{-1}
10^{-2}
10^{-3}
5
10
20
50
100
200
300
2
4
6
8
10
12
14
16
18
20
22

Figure 2

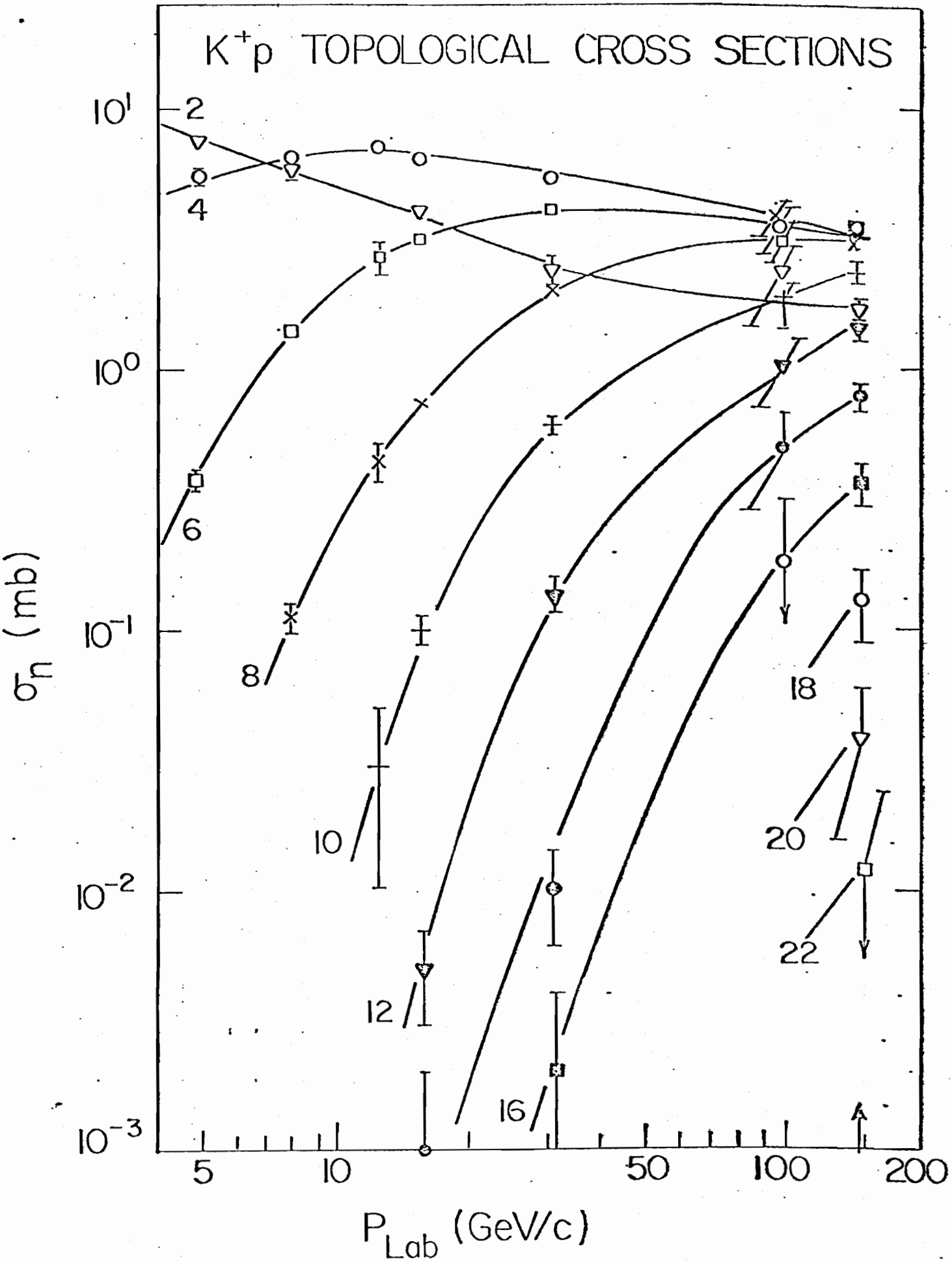
K⁺p TOPOLOGICAL CROSS SECTIONS
10^1
10^0
10^{-1}
10^{-2}
10^{-3}
σ_n (mb)
2
4
6
8
10
12
16
18
20
22
5
10
50
100
200
P_{Lab} (GeV/c)

Figure 3

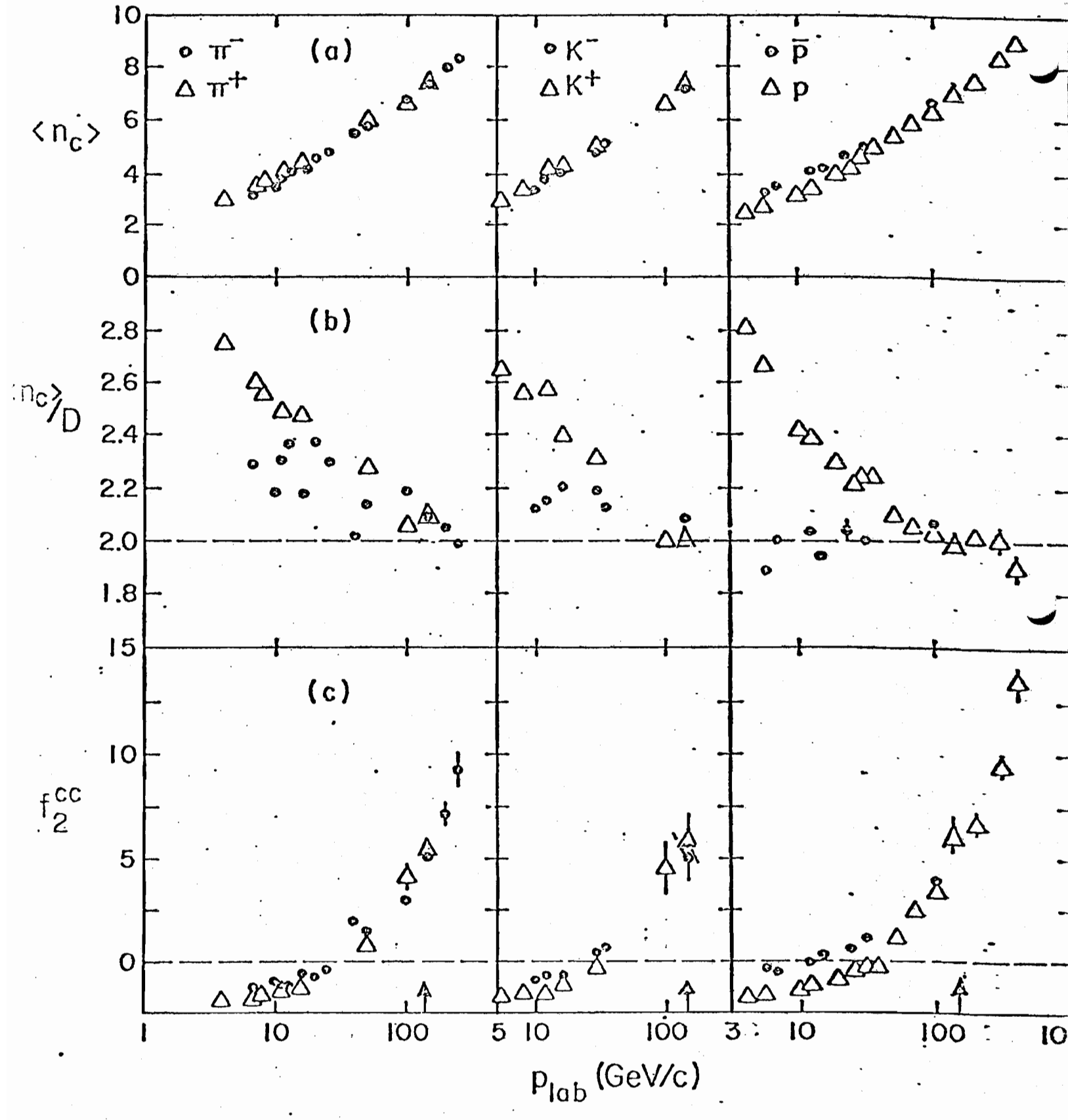
(a)
(b)
(c)
π^-
π^+
K^-
K^+
$\bar{p}$
p
$\langle n_c \rangle$
$\langle n_c \rangle / D$
f_2^{cc}
p_{lab} (GeV/c)

Figure 4

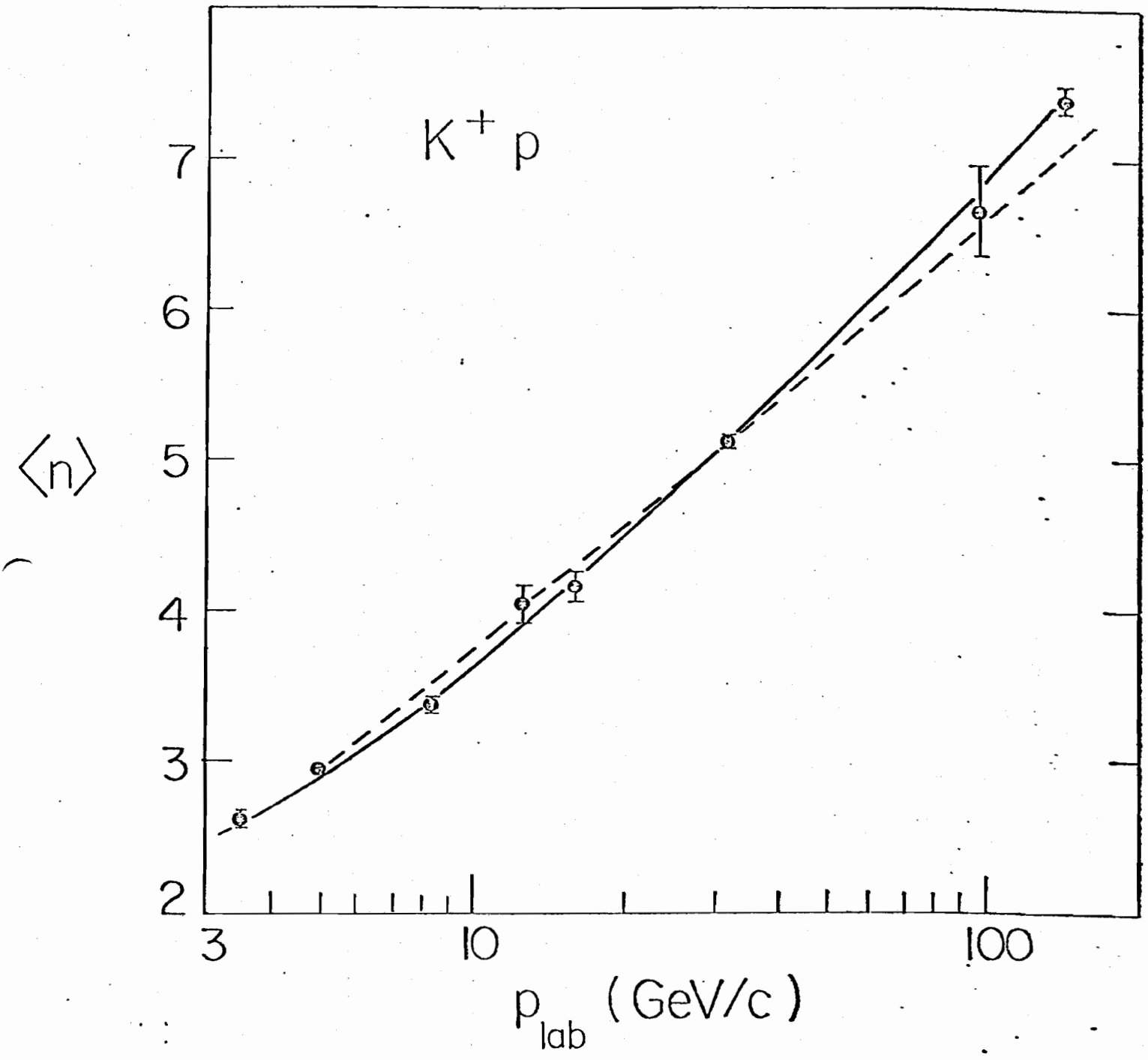

Figure 5

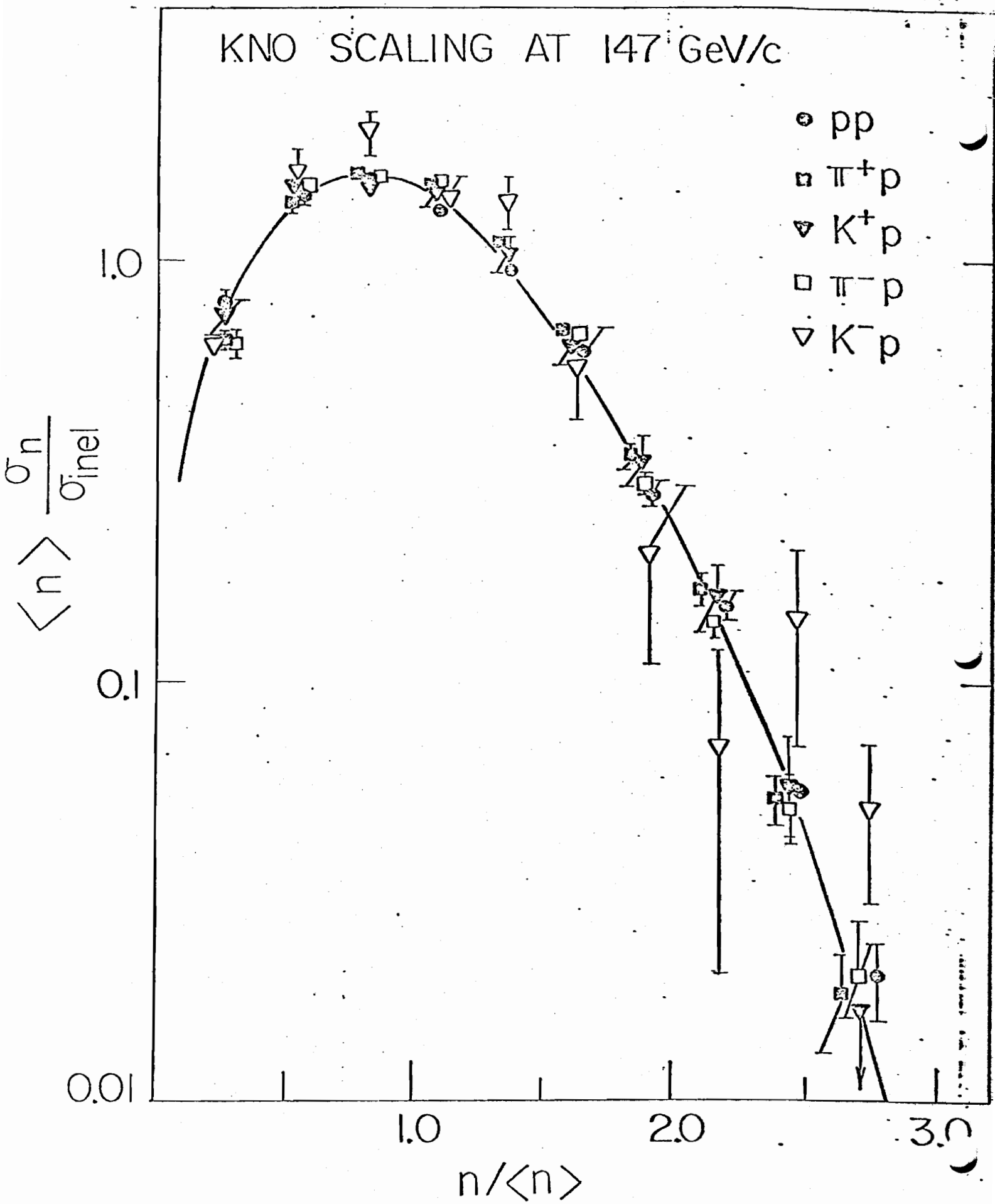
KNO SCALING AT 147 GeV/c
pp
π⁺p
K⁺p
π⁻p
K⁻p
1.0
0.1
0.01
⟨n⟩ σn/σinel
1.0
2.0
3.0
n/⟨n⟩

Figure 6